

This document contains a post-print version of the paper

Extension and optimization of the load range of DRT test systems for testing extra-long HV and UHV cables

authored by **P. Mohaupt, H. Geyer, B. A. Bergmann, S. Bergmann, E. Bergmann, W. Kemmetmüller, S. Eberharter, and A. Kugi**

and published in *e & i Elektrotechnik und Informationstechnik*.

The content of this post-print version is identical to the published paper but without the publisher's final layout or copy editing. Please, scroll down for the article.

Cite this article as:

P. Mohaupt, H. Geyer, B. A. Bergmann, S. Bergmann, E. Bergmann, W. Kemmetmüller, S. Eberharter, and A. Kugi, "Extension and optimization of the load range of drt test systems for testing extra-long hv and uhv cables", *e & i Elektrotechnik und Informationstechnik*, vol. 130, pp. 1–5, Jan. 2013. doi: [10.1007/s00502-012-0109-x](https://doi.org/10.1007/s00502-012-0109-x)

BibTex entry:

```
@ARTICLE{eberharter_2013,
  author = {P. Mohaupt and H. Geyer and B. A. Bergmann and S. Bergmann and E. Bergmann and W. Kemmetm\"uller and S. Eberharter and A. Kugi},
  title = {Extension and optimization of the load range of DRT test systems for testing extra-long HV and UHV cables},
  journal = {e \& i Elektrotechnik und Informationstechnik},
  year = {2013},
  volume = {130},
  pages = {1-5},
  month = {January},
  doi = {10.1007/s00502-012-0109-x},
  url = {http://link.springer.com/article/10.1007%2Fs00502-012-0109-x}
}
```

Link to original paper:

<http://dx.doi.org/10.1007/s00502-012-0109-x>
<http://link.springer.com/article/10.1007/s00502-012-0109-x>

Read more ACIN papers or get this document:

<http://www.acin.tuwien.ac.at/literature>

Contact:

Automation and Control Institute (ACIN)
Vienna University of Technology
Gusshausstrasse 27-29/E376
1040 Vienna, Austria

Internet: www.acin.tuwien.ac.at
E-mail: office@acin.tuwien.ac.at
Phone: +43 1 58801 37601
Fax: +43 1 58801 37699

Copyright notice:

The final publication is available at <http://dx.doi.org/10.1007/s00502-012-0109-x>

Extension and optimization of the load range of DRT test systems for testing extra-long HV and UHV cables

P. Mohaupt, H. Geyer, B. A. Bergman, S. Bergman, A. E. Bergman, W. Kemmetmüller, S. Eberharter, A. Kugi OVE

In the last few years, the demand for testing extra-long cables, such as submarine cables has grown rapidly. The existing testing methods have been complemented by a new testing technology called DRT (Differential Resonance Technology). This testing method enables testing of extra-long cables by comparably small and light-weight equipment using a low frequency for the test voltage, e.g. 0.1 Hz up to 5 Hz. This leads to a significant decrease of the required power of the test source (P. Mohaupt and A. Bergman in CIGRE 2010).

In a resonant circuit only the losses of the generator's individual components, specifically the high voltage reactor, have to be covered by the mains. The testing power itself remains fully compensated. Typical ratios between the testing power and the input power of resonant test systems start at 50 and go up to 100, depending on the load. Unfortunately, voltage generation based on inductive generation principles such as resonant circuits cannot economically be used for frequencies below 10 Hz due to the massive iron cores needed for such a low frequency.

The DRT method for the generation of low frequency high voltage is based on a high frequency voltage whose amplitude is modulated by the desired low frequency. Using a resonator, which is tuned to the high frequency, and a demodulator, the desired low frequency high voltage can be generated (P. Mohaupt and A. Bergman in CIGRE 2010; P. Mohaupt and T. Mehl in Jicable 2011). The input power required—and in direct relation to this the size and weight of the equipment—is significantly smaller than for other existing methods. In order to optimize the operation performance of the DRT system, this paper describes mathematical methods and algorithms, which have already been implemented and tested in a DRT test set. The basis for these algorithms is a mathematical description of the system based on an envelope model. Using this mathematical description of the nonlinear system behavior, a systematic analysis of the performance and the limits of the system can be given.

The theoretical approach was experimentally proven by measuring the output voltage and the input power of a prototype unit ultimately designed to produce 200 kVrms. A first test was performed at SP Technical Research Institute of Sweden, using their reference measurement system for very low frequency (VLF) S. Bergman and A. Bergman (Proc. CPEM Conf. Dig., pp. 682–683, 2010; IEEE Trans. Instrum. Meas. 60:2422–2426, 2011) to measure the high VLF voltage. The reference measurement system provides a traceable uncertainty of down to 0.04 % over a voltage range up to 200 kV rms. The frequency range of the reference system is from 0.1 Hz up to 50 Hz. This system permits acquisition of complete wave-forms that can be analysed for harmonic content and/or THD (Total Harmonic Distortion).

Further tests are planned, where the connected load will be increased to the specified maximum 1 μ F at 200 kV, and the characteristics will be explored both as regards to output voltage quality, input power requirements and distortion on the input current.

Keywords: cable testing; on-site testing; VLF; very low frequency; variable frequency resonant test system; testing of sea cables; DRT

© CIGRE – Reprint from www.cigre.org with kind permission 2013

1. Introduction

An increasing demand for testing long and extra-long HV and UHV cables such as submarine cables can be noticed. The so far established test technique using a variable frequency resonant circuit comes to its limit in size, weight and handling. A new testing technology based on DRT was recently presented by the authors in Mohaupt and Bergman (2010), Mohaupt and Mehl (2011), Bergman and Bergman (2011). This testing technology has now been proven for a first unit intended for field operation up to 200 kV (see Fig. 1).

In Fig. 2, the basic working principle of a DRT system is presented. The capacitive load (test object) is charged by a sinusoidal beat frequency oscillation (BFO) over a demodulator setup (switched valve unit—SVU). The beat frequency oscillation consists of the carrier frequency in the range of 1 kHz, whose amplitude is modulated by the desired test frequency of, e.g., 0.1 Hz or higher. Therein, a resonant circuit tuned to the carrier frequency allows for the simple generation of the necessary high voltages. The output frequency can be easily changed in the range from 0.1 Hz

up to 5 or even 10 Hz by changing the modulation frequency. Higher frequencies, however, require a higher input power of the system which implies that the system components need to be designed for that. The patented (Patent WO PCT/AT09/00211 00 2010; Patent WO PCT/AT09/00212 00 2010) working principle of a DRT system is described in more detail in Mohaupt and Bergman (2010), Mohaupt and Mehl (2011).

In addition, the DRT system has the possibility of testing at DC, enabling a charging of the load capacity with a charging current of up to 16 A. Discharging after the test is accomplished by controlled

Paper submitted for the CIGRE Session 2012, SC B1, Paris, France, August 27–31, 2012.

Mohaupt, P., Mohaupt High Voltage GmbH, Mieders, Austria
 (E-mail: peter.mohaupt@mohaupt-hv.com); **Geyer, H.**, Mohaupt High Voltage GmbH, Mieders, Austria; **Bergman, B. A.**, SP Sweden, Borås, Sweden; **Bergman, S.**, SP Sweden, Borås, Sweden; **Bergman, A. E.**, SP Sweden, Borås, Sweden; **Kemmetmüller, W.**, Vienna University of Technology, Vienna, Austria; **Eberharter, S.**, Vienna University of Technology, Vienna, Austria; **Kugi, A.**, Vienna University of Technology, Vienna, Austria

discharging with the same constant current. This can be realised in one system together with a standard DRT setup.

The future challenge of DRT systems is to optimize—apart from size and weight—the input power and the shape of the test voltage as treated in IEC 60060-1 (2010), IEC 60060-2 (2010), even though, so far these standards do not cover sinusoidal voltage of a frequency lower than 10 Hz. Therefore, the focus of this paper is put on the optimization of the input power and the distortion of the voltage shape. The distortion of the voltage shape is frequently measured by means of the THD. However in terms of high voltage measure-

ment the THD is not the relevant quantity but the ratio of the peak value divided by square root of 2 to the RMS value of the voltage signal is important. Practical measurements show that the THD is a more severe criterion compared to the ratio of peak/sqrt(2) to RMS value, as defined in IEC 60060-1 (2010). The main component influencing those factors (input power and distortion of the voltage shape) is the demodulator, also called Switch Valve Unit (SVU). The optimization is based on a detailed mathematical description of the system. Therefore, both the mathematical modelling and the optimization will be described in detail in this contribution.

2. Mathematical model

This section is concerned with the mathematical model of the DRT system. As already mentioned before, the mathematical model is the basis for the analysis and the optimization of the system behavior. Furthermore, the mathematical model allows to simulate different system configurations and control strategies. Due to limited space a very condensed version of the mathematical model will be given. A detailed description can be found in Kemmetmüller and Kugi (2012).

The equivalent circuit diagram of the DRT system is shown in Fig. 3. Therein, the demodulator is described by a variable resistor $R_{dm}(t)$. By means of a defined switching sequence of the SVU thyristors, the value of $R_{dm}(t)$ can be varied between R_{on} and R_{off} .

The exciter is supplied by the tuneable voltages of the power module u_{p1} and u_{p2} . The corresponding currents i_{p1} , i_{p2} and the resonator current i_r can be described by the following differential equation

$$\mathbf{L} \frac{d}{dt} \begin{bmatrix} i_{p1} \\ i_{p2} \\ i_r \end{bmatrix} = \begin{bmatrix} -R_p i_{p1} + u_{p1} \\ -R_p i_{p2} + u_{p2} \\ -(2R_s + R_r)i_r + u_z \end{bmatrix} \quad (1)$$

where R_r is the resistance of the resonator circuit, R_p and R_s are the primary and secondary resistances of the exciter and u_z is the voltage of the resonator capacity. The inductance matrix \mathbf{L} is given by

$$\mathbf{L} = \begin{bmatrix} L_p & 0 & L_{ps} \\ 0 & L_p & L_{ps} \\ L_{ps} & L_{ps} & 2L_s + L_r \end{bmatrix}, \quad (2)$$

with the primary and secondary inductances of the exciter L_p and L_s , respectively, the resonator inductance L_r and the coupling inductance L_{ps} which can be given by $L_{ps} = k\sqrt{L_p L_s}$ with the coupling factor $k < 1$. The differential equations of the output voltage u_i and the voltage of the resonator capacity u_z can be written as

$$\frac{d}{dt} u_z = \frac{1}{C_r} (-i_r - i_{dm}) \quad (3a)$$



Fig. 1. On Site Test System DRT200-1, 200 kV, 1 μ F

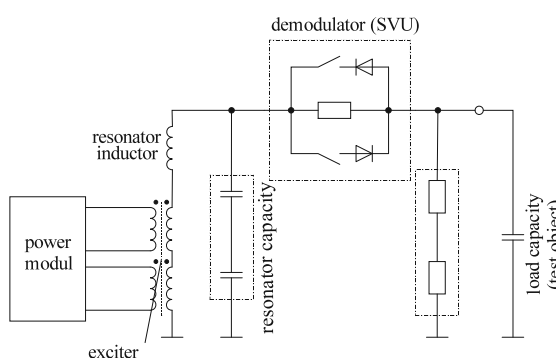


Fig. 2. Working principle DRT system

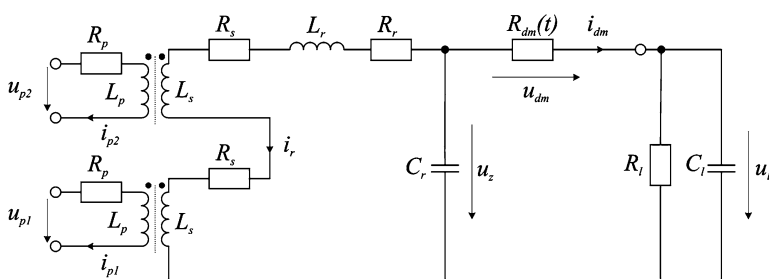


Fig. 3. Equivalent circuit diagram of the DRT system

$$\frac{d}{dt}u_I = \frac{1}{C_I} \left(-\frac{u_I}{R_I} + i_{dm} \right). \quad (3b)$$

Here, i_{dm} describes the demodulator current which is calculated by

$$i_{dm} = \frac{1}{R_{off}} u_{dm} + \left(\frac{1}{R_{dm}^+} - \frac{1}{R_{off}} \right) g^+ + \left(\frac{1}{R_{dm}^-} - \frac{1}{R_{off}} \right) g^- \quad (4a)$$

$$g^+ = \begin{cases} u_{dm} & |u_{dm}| \geq 0 \\ 0 & |u_{dm}| < 0 \end{cases} \quad (4b)$$

$$g^- = \begin{cases} 0 & |u_{dm}| \geq 0 \\ u_{dm} & |u_{dm}| < 0 \end{cases} \quad (4c)$$

with the resistance of the positive and negative thyristor branch R_{dm}^+ and R_{dm}^- as well as the demodulator voltage $u_{dm} = u_z - u_I$. The values of R_{dm}^+ and R_{dm}^- can be actively changed by a suitable switching sequence of the demodulator thyristors.

3. Envelope model

Based on this mathematical model an envelope model is developed, which is better suited for the analysis and the optimization of the DRT system. For the derivation of the envelope model, a reduced model is obtained by the regular state transformation $i_\Sigma = i_{p1} + i_{p2}$, $i_\Delta = i_{p1} - i_{p2}$ with the new system inputs $u_\Sigma = u_{p1} + u_{p2}$ and $u_\Delta = u_{p1} - u_{p2}$, see Kemmetmüller and Kugi (2012) for more details.

The main idea of the envelope model is to approximate the system's state variables by a slowly time varying mean value $X_0(t)$, a cosine value $X_c(t)\cos(\omega_r t)$ and a sine value $X_s(t)\sin(\omega_r t)$, i.e.

$$x(t) = X_0(t) + X_c(t)\cos(\omega_r t) + X_s(t)\sin(\omega_r t) \quad (5)$$

where ω_r is the carrier frequency. With this, the time derivative of state variables can be written as

$$\dot{x} = \dot{X}\mathbf{w} + X\dot{\mathbf{w}} \quad (6)$$

with

$$\mathbf{X} = [X_0(t) \ X_c(t) \ X_s(t)], \quad \mathbf{w} = \begin{bmatrix} 1 \\ \cos(\omega_r t) \\ \sin(\omega_r t) \end{bmatrix} \quad (7)$$

and

$$\dot{\mathbf{w}} = \begin{bmatrix} 0 & 0 & 0 \\ 0 & 0 & -\omega_r \\ 0 & \omega_r & 0 \end{bmatrix} \begin{bmatrix} 1 \\ \cos(\omega_r t) \\ \sin(\omega_r t) \end{bmatrix} = \Omega \mathbf{w}. \quad (8)$$

Using (5)–(8), the resulting differential equations of the envelope model are given by Kemmetmüller and Kugi (2012)

$$\mathbf{L}_{\Sigma,r} \frac{d}{dt} \begin{bmatrix} \mathbf{I}_\Sigma \\ \mathbf{I}_r \end{bmatrix} = -\mathbf{L}_{\Sigma,r} \begin{bmatrix} \mathbf{I}_\Sigma \\ \mathbf{I}_r \end{bmatrix} \Omega - \begin{bmatrix} R_p & 0 \\ 0 & 2R_s + R_r \end{bmatrix} \begin{bmatrix} \mathbf{I}_\Sigma \\ \mathbf{I}_r \end{bmatrix} + \begin{bmatrix} \mathbf{U}_\Sigma \\ \mathbf{U}_r \end{bmatrix} \quad (9a)$$

$$L_p \frac{d}{dt} \mathbf{I}_\Delta = -L_p \mathbf{I}_\Delta \Omega - R_p \mathbf{I}_\Delta + \mathbf{U}_\Delta \quad (9b)$$

$$\frac{d}{dt} \mathbf{U}_z = -\mathbf{U}_z \Omega + \frac{1}{C_r} (-\mathbf{I}_r - \mathbf{I}_{dm}) \quad (9c)$$

$$\frac{d}{dt} \mathbf{U}_I = -\mathbf{U}_I \Omega + \frac{1}{C_I} \left(-\frac{\mathbf{U}_I}{R_I} + \mathbf{I}_{dm} \right), \quad (9d)$$

with the reduced inductance matrix

$$\mathbf{L}_{\Sigma,r} = \begin{bmatrix} L_p & 2L_{ps} \\ L_{ps} & 2L_s + L_r \end{bmatrix}. \quad (10)$$

4. Discharge control of the output voltage

In case of AC operation, the goal of the DRT system is to apply a low frequency sinusoidal voltage to the capacitive load (test object). Thus, the load needs to be charged and discharged according to the desired (sinusoidal) shape of the output voltage in terms of the requested THD and in accordance with IEC 60060-1 (2010).

For this purpose, there are basically two control inputs in the system: (i) the voltage u_z of the resonator capacity¹ and (ii) the resistances R_{dm}^+ and R_{dm}^- of the demodulator.

The standard control strategy for the DRT system is to switch on the positive part of the demodulator for the positive half-wave ($R_{dm}^+ = R_{on}$, $R_{dm}^- = R_{off}$) and the negative part of the demodulator for the negative half-wave ($R_{dm}^+ = R_{off}$, $R_{dm}^- = R_{on}$). Furthermore, the amplitude of the voltage u_z is chosen according to the desired amplitude of the voltage on the test object. This standard control strategy works well for small and medium load capacities. For large capacitive loads, however, significant errors do occur especially during the discharge phase of the load. This is basically due to the fact that the discharge of the load (i.e. the slope of the load voltage) is limited by the resistance of the demodulator. During the positive half-wave, the value $R_{dm}^- = R_{off}$ of the negative part of the demodulator defines the maximum slope of the load voltage. If this slope is lower than the slope of the desired load voltage (i.e. the load is discharged too slow), an error occurs between the desired and the actual value of the voltage, cf. Fig. 4a.

Based on the envelope model (9a)–(9c) an analytical expression for the minimal output voltage up to which it is possible to track the desired voltage without error can be found in the form Kemmetmüller and Kugi (2012)

$$u_{I,min} = \hat{u}_I - \frac{1}{\sqrt{\left(\frac{1}{R_I} + \frac{1}{R_{off}}\right)^2 + 1}}, \quad (11)$$

where $\Delta\omega$ is the frequency of the output voltage u_I and R_I is the resistance of the test object. Starting from this value, the load capacity is then discharged according to

$$\frac{d}{dt} u_I = -\frac{1}{C_I} \left(\frac{1}{R_I} + \frac{1}{R_{off}} \right) u_I, \quad u_I(t_{I,min}) = u_{I,min}. \quad (12)$$

A simple analysis shows that for large values of C_I the minimum voltage $u_{I,min}$ becomes rather large such that the demands on the quality of the output voltage can no longer be reached.

Therefore, two alternative methods for the discharge control have been developed:

- Block control (strategy b): In this strategy, the value of the discharge resistance R_{off} is lowered by short circuiting blocks of the SVU setup.
- Counter control (strategy c): The capacitive load is actively connected to the negative value of the BFO voltage u_z to achieve a higher voltage gradient for discharging compared to discharging to the ground potential.

Block control: The demodulator is divided into several blocks. Using a suitable control setup, the resistance of the individual blocks for discharging the load capacity can be gradually reduced by defined switching sequences of the SVU thyristors (see t_{s1} , t_{s2} in Fig. 4b). With this type of control, medium to high capacities can be tested. The accuracy of the output voltage is, however, limited

¹Of course, the voltage at the resonator capacity cannot be directly impressed. It is, however, rather simple to adjust this voltage by means of the voltages u_{p1} and u_{p2} of the power module.

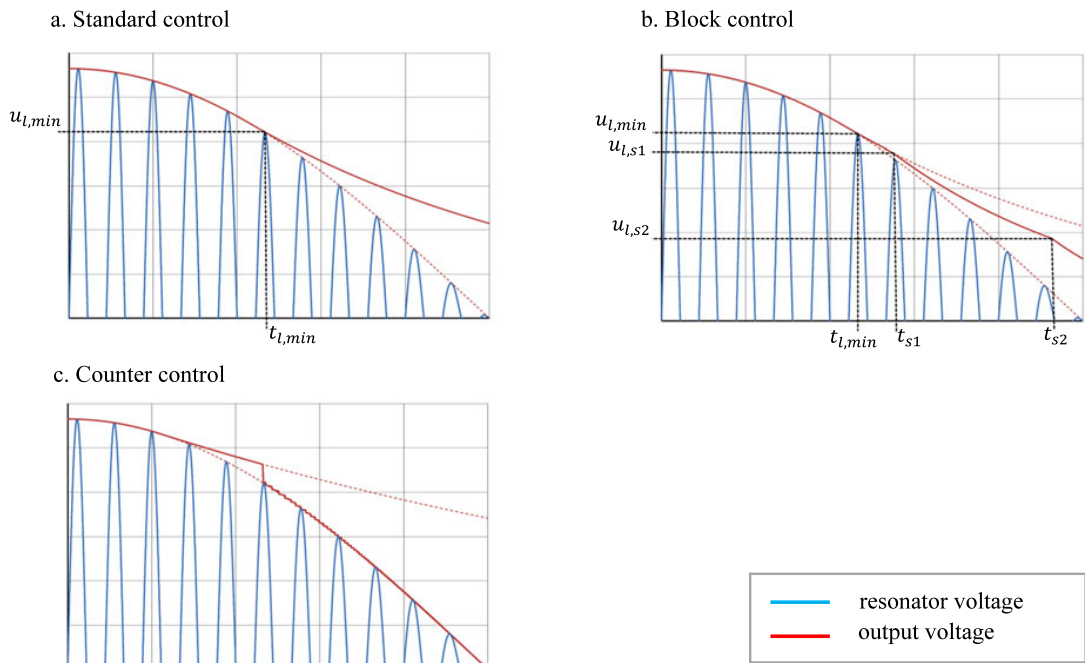


Fig. 4. Overview of the different types of discharge control. a. Standard control using a constant discharge resistor. b. Block control using blocks of discharge resistors: Each individual block section follows an exponential discharge voltage shape. c. Counter control using the voltage potential of the opposite polarity for discharging

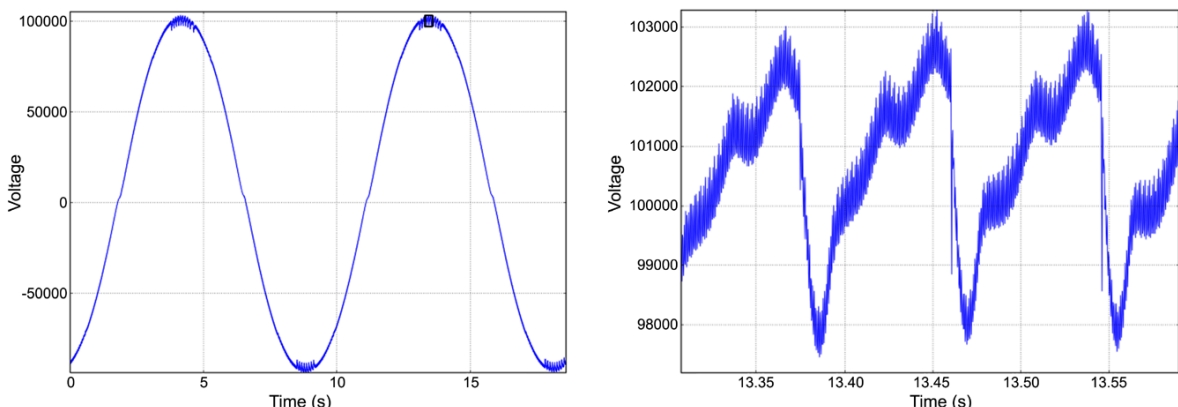


Fig. 5. 70 kV RMS overview zoom on peak distortions

by the number of blocks of the demodulator and the corresponding withstand voltage of the thyristors.

Counter control: The above drawbacks of the standard control and the block control concerning the accuracy of the output voltage can be improved for long and very long cables (i.e. for large values of the load capacity) by switching on the negative part of the demodulator for short periods in the positive half-wave. Doing so, the slope of the load voltage can be adjusted to the desired slope such that rather small errors of the output voltage can be reached (see Fig. 4c). There is, however, the need for a very exact timing of the switching sequence of the negative part of the demodulator.

5. Measurement results at SP

The output voltage of the DRT system was measured using SP's reference measurement system consisting of a capacitive voltage divider, a HP3458 DMM and dedicated measuring cables. The capacitive voltage divider used a 300 kV compressed gas capacitor at 50 pF and a low voltage capacitor consisting of an array of NPO ceramic capacitors at a total of 2.5 μ F. The frequency dependence of the low voltage arm was compensated for. The frequency dependence of the high voltage arm is negligible. The 0.1 Hz output waveform was sampled with 75000 samples taken over 1 up to 5 cycles of the DRT system's output using a HP3458 DMM. The load on the test object was varied from a few hundred pF, when the only load

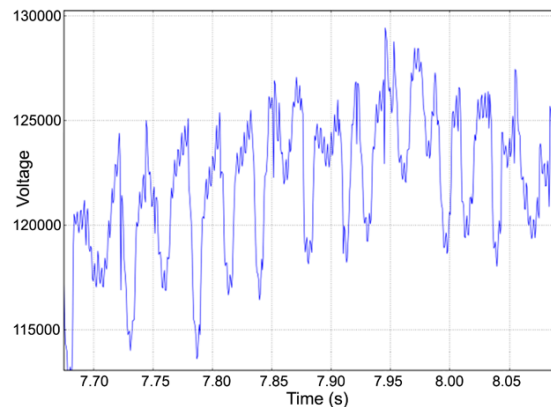
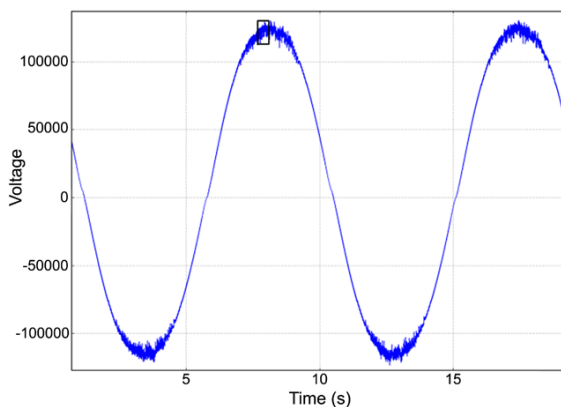


Fig. 6. 90 kV RMS overview zoom on peak distortions

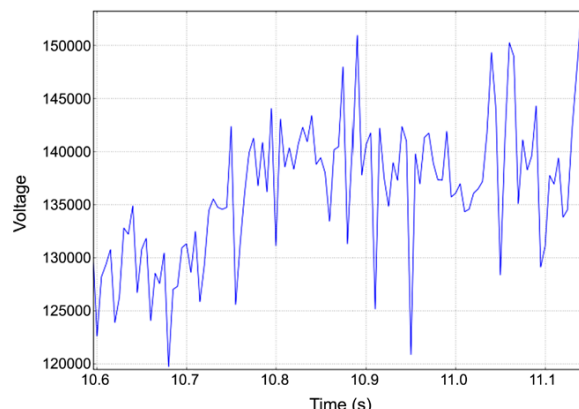
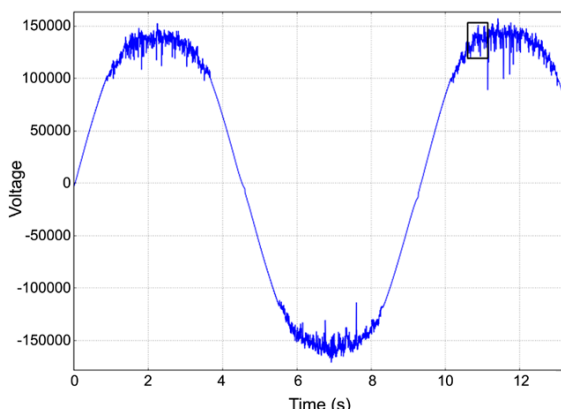


Fig. 7. 100 kV RMS overview zoom on peak distortions, low time resolution

was the measurement system and up to 6 nF, adding high voltage capacitors.

The system showed some instabilities at output voltages above 70 kV RMS, above which the voltage experienced sudden drops and recoveries of voltage. When the voltage is only slightly above 70 kV RMS the voltage drops occurred at approximately 10 Hz and at increasing voltages the frequency and distortion of the voltage drops increase. The THD at 70 kVRMS was approximately 1.5 %. Figures 5, 6, 7 depict plots of the output voltage at 70 kV, 90 kV and 100 kV. The distortion levels of the peaks are 5.6 kV, 9 kV and 16 kV, respectively.

Additionally, the harmonic content of the mains current was analyzed. The fifth harmonic on the input of the DRT varied from 40–60 % of the fundamental at 100 kV RMS and the seventh harmonic varied between 15–45 %. The third harmonic was below 20 % of the fundamental at all times. The current drawn from the mains changes greatly with a frequency of 0.2 Hz, which corresponds to the frequency of the output voltage.

6. Conclusion

A new testing method for testing long and extra-long high voltage cables, called Differential Resonance Technology (DRT) is presented.

The working principle and the challenges for discharging high capacitive loads at high voltages are described. Especially the mathematical model and the limits of the discharge control and different approaches for discharge control discussed. Measurements of the input power and the voltage shape were performed at SP Sweden.

References

- Bergman, S., Bergman, A. (2010): New reference measurement system for calibration of VLF high voltage. In Proc. CPEM conf. dig. (pp. 682–683).
- Bergman, S., Bergman, A. (2011): New reference measurement system for calibration of VLF high voltage. IEEE Trans. Instrum. Meas., 60(7), 2422–2426.
- IEC 60060-1 (2010).
- IEC 60060-2 (2010).
- Kemmetmüller, W., Kugi, A. (2012): Mathematical modeling and analysis of a DRT-VLF high voltage test generator. e&i – Elektrotechnik und Informationstechnik. doi:[10.1007/s00502-012-0073-5](https://doi.org/10.1007/s00502-012-0073-5).
- Mohaupt, P., Bergman, A. (2010): A new concept for test equipment for testing large HV and UHV cables on-site. In CIGRE 2010, Paris. Paper B1_302_2010.
- Mohaupt, P., Mehl, T. (2011): A new approach for testing long HV and UHV cables. In Jicable 2011, Versailles. Paper 0116 A.8.4.
- Patent WO PCT/AT09/00211 00 (2010): VLF test generator.
- Patent WO PCT/AT09/00212 00 (2010): VLF test generator.